University of Ioannina
Department of Physics

- Improvement of PCM performances by means of nanoparticle (NP) additions (Task 2.1).

- Development of a ALN based thin film to protect the HEs metal surface from the corrosion of Hydrated salts (Task 3.3).

Procedure:

- Improvement of PCM performances by means of nanoparticle (NP) additions.
    - Selection of suitable nanoparticles.
    - Construction of a safe environment for nanoparticles manipulation.
    - Development of T-History equipment + software.
    - Testing and calibration of equipment and software on standard PCM substances
    - Development of alternative method
    - Evaluations of thermal properties actual PCMs + NP additions

T-History Curve for Lauric Acid

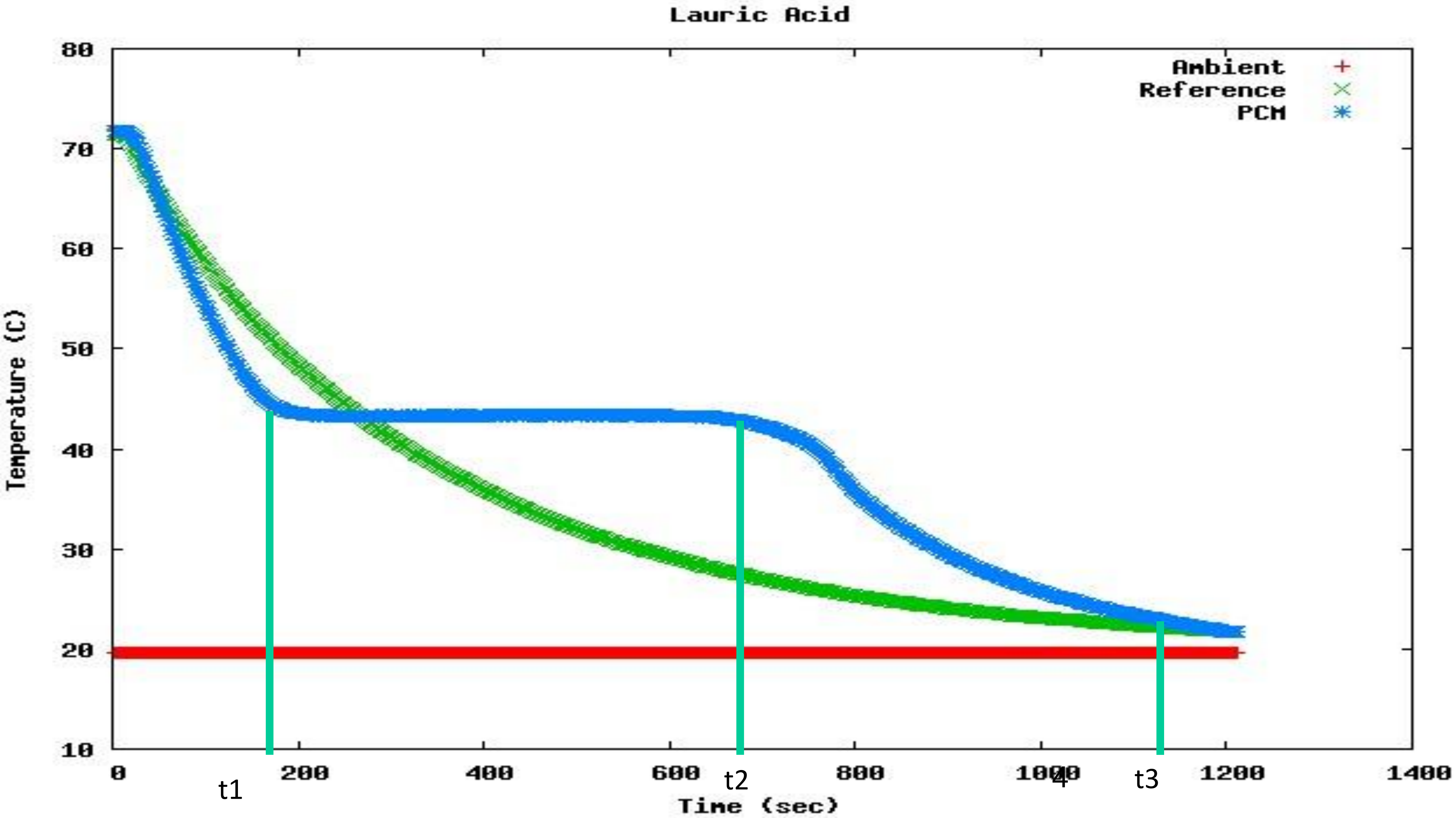

Lauric Acid: Enthalpy vs Temperature

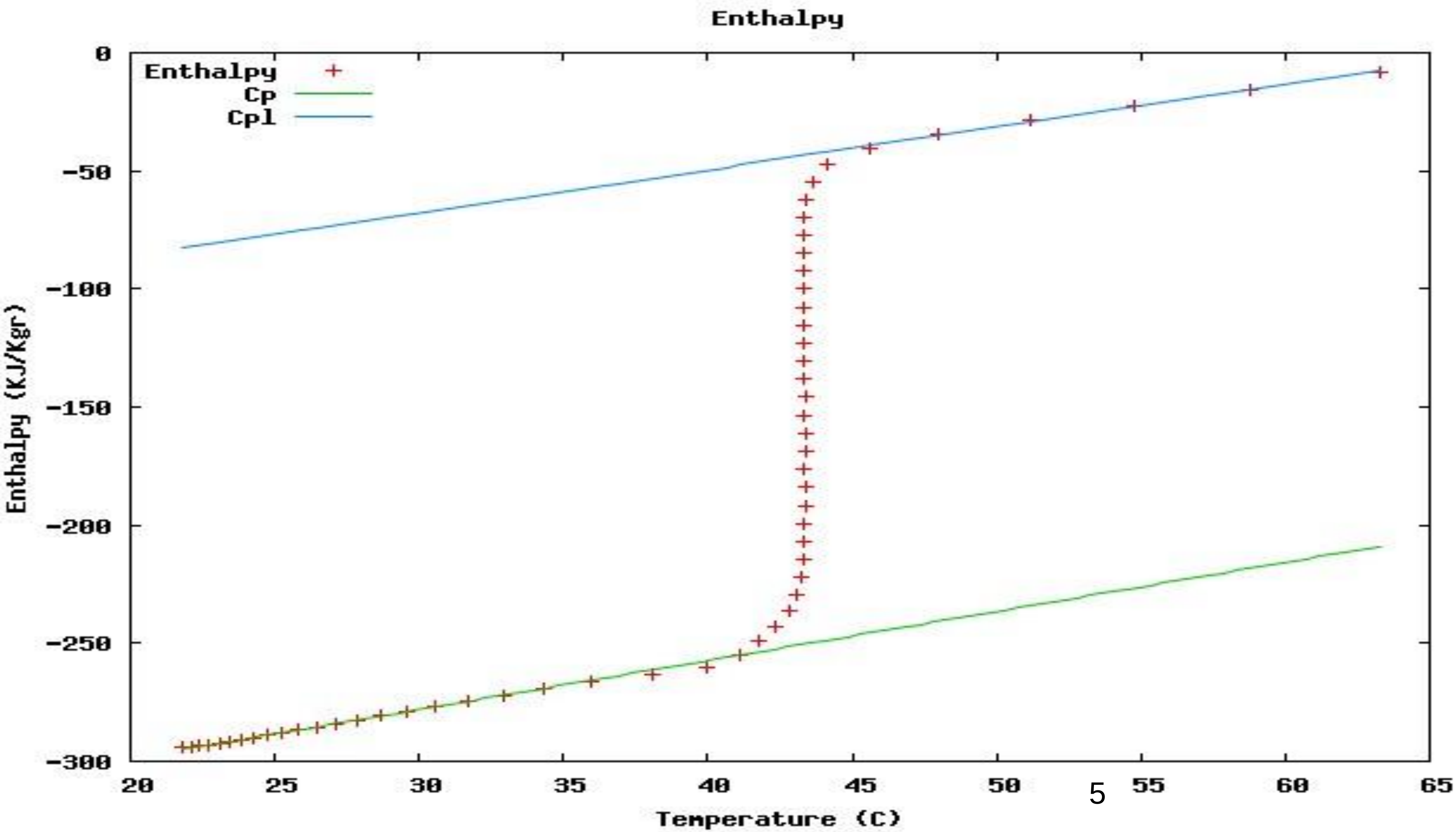

Lauric Acid: Specific Heat vs Temperature

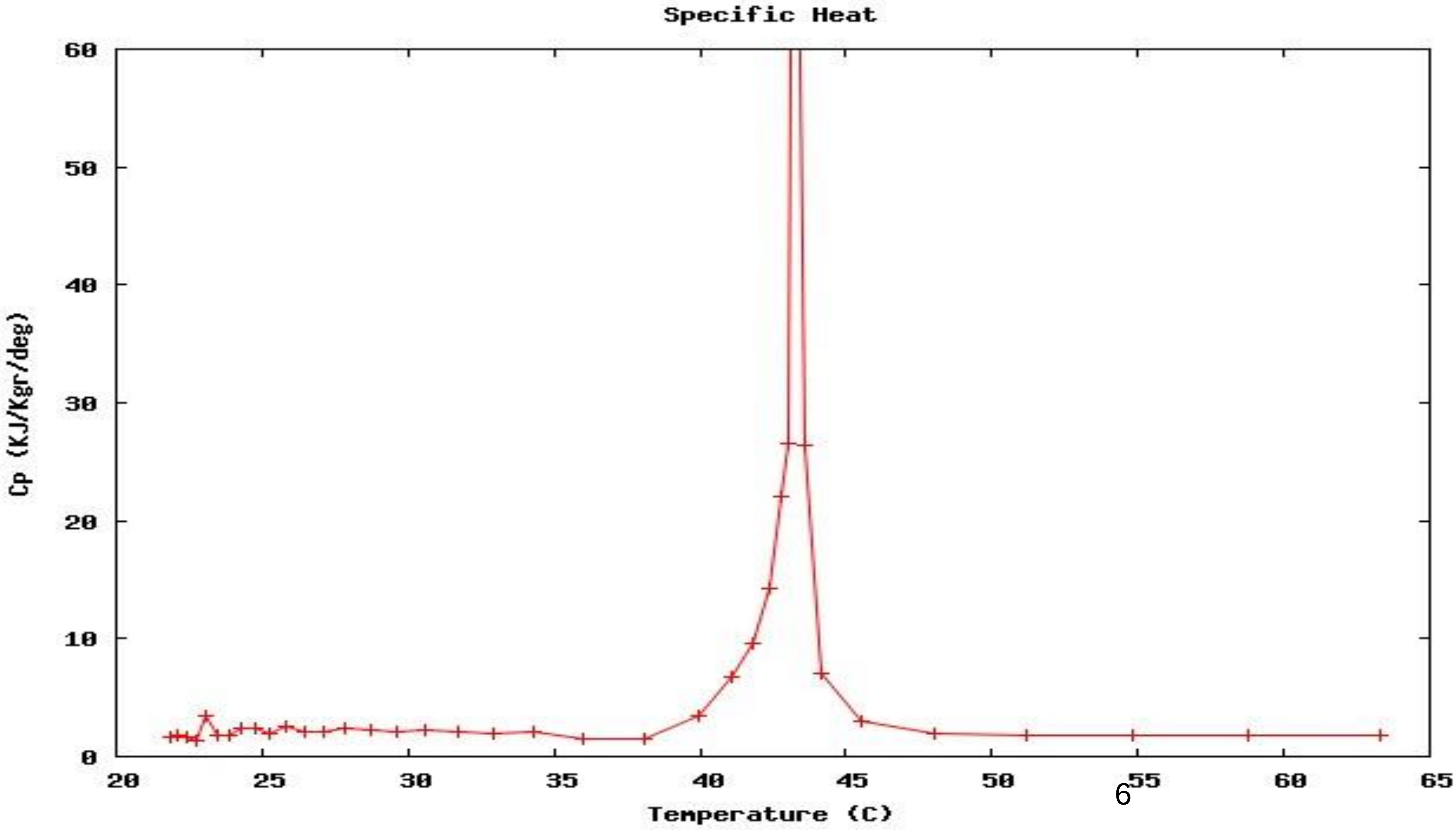

T-History curve for A53 PCM

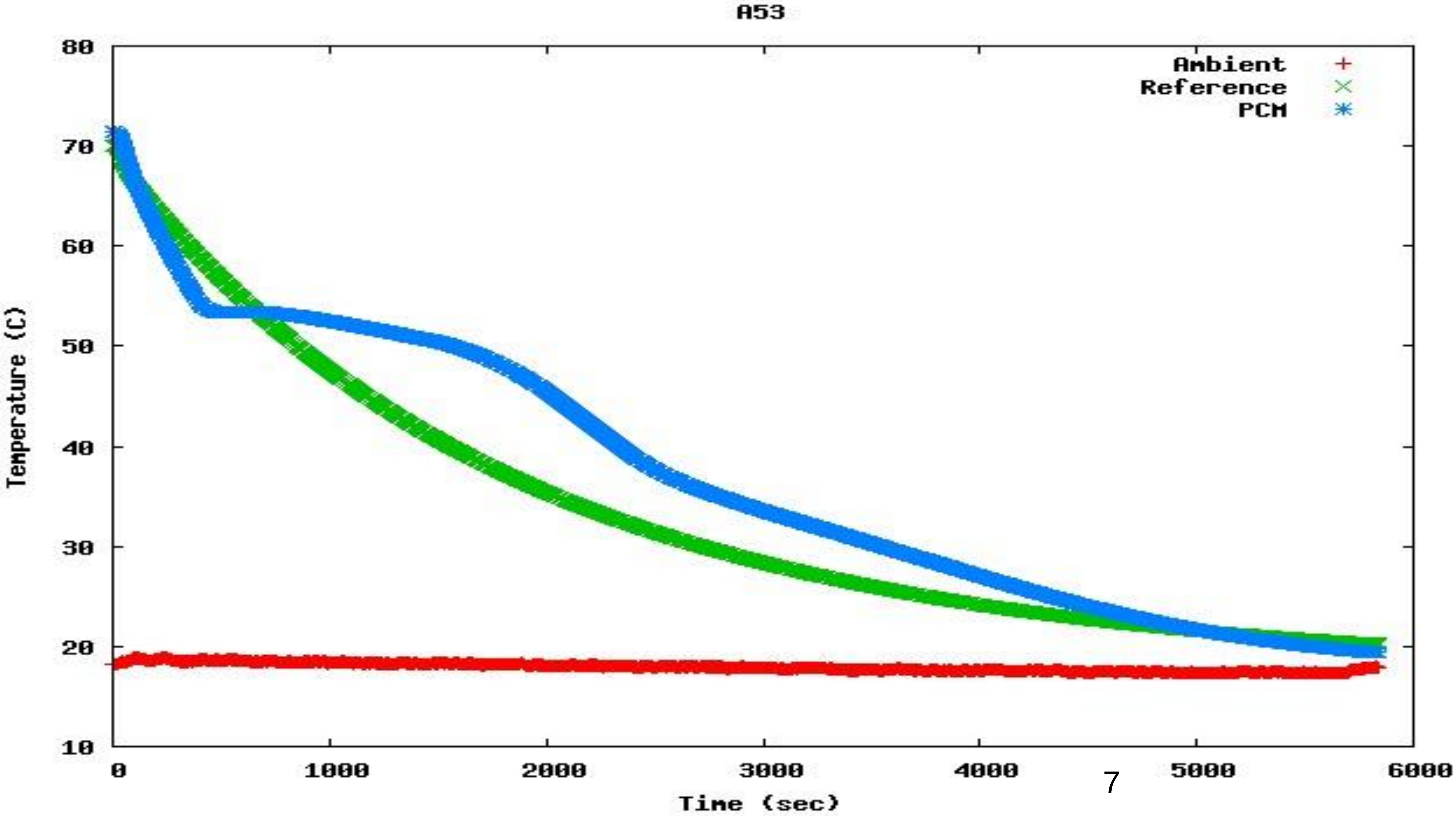

A53 Supercooled region

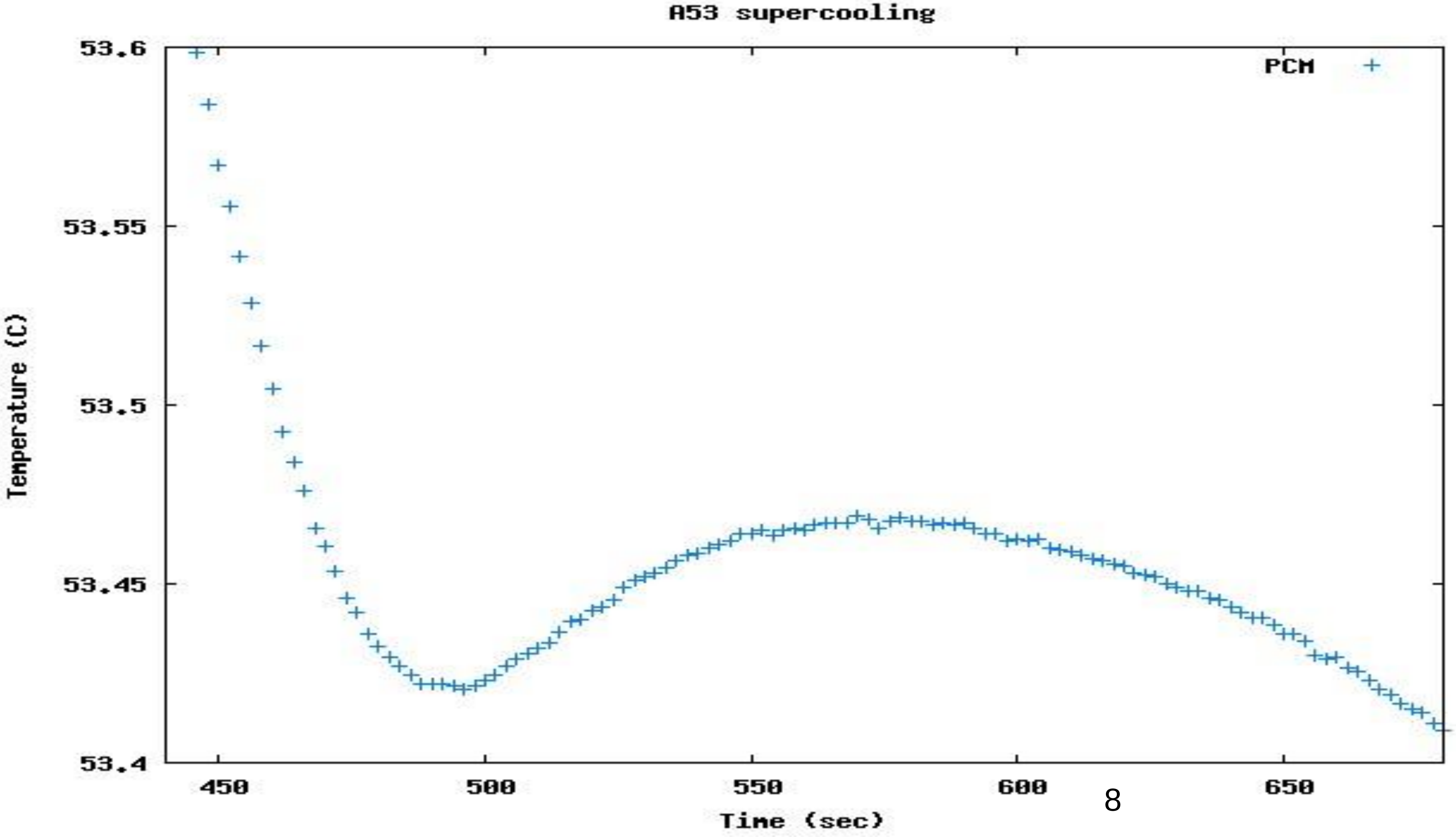

A53 Enthalpy vs Temperature

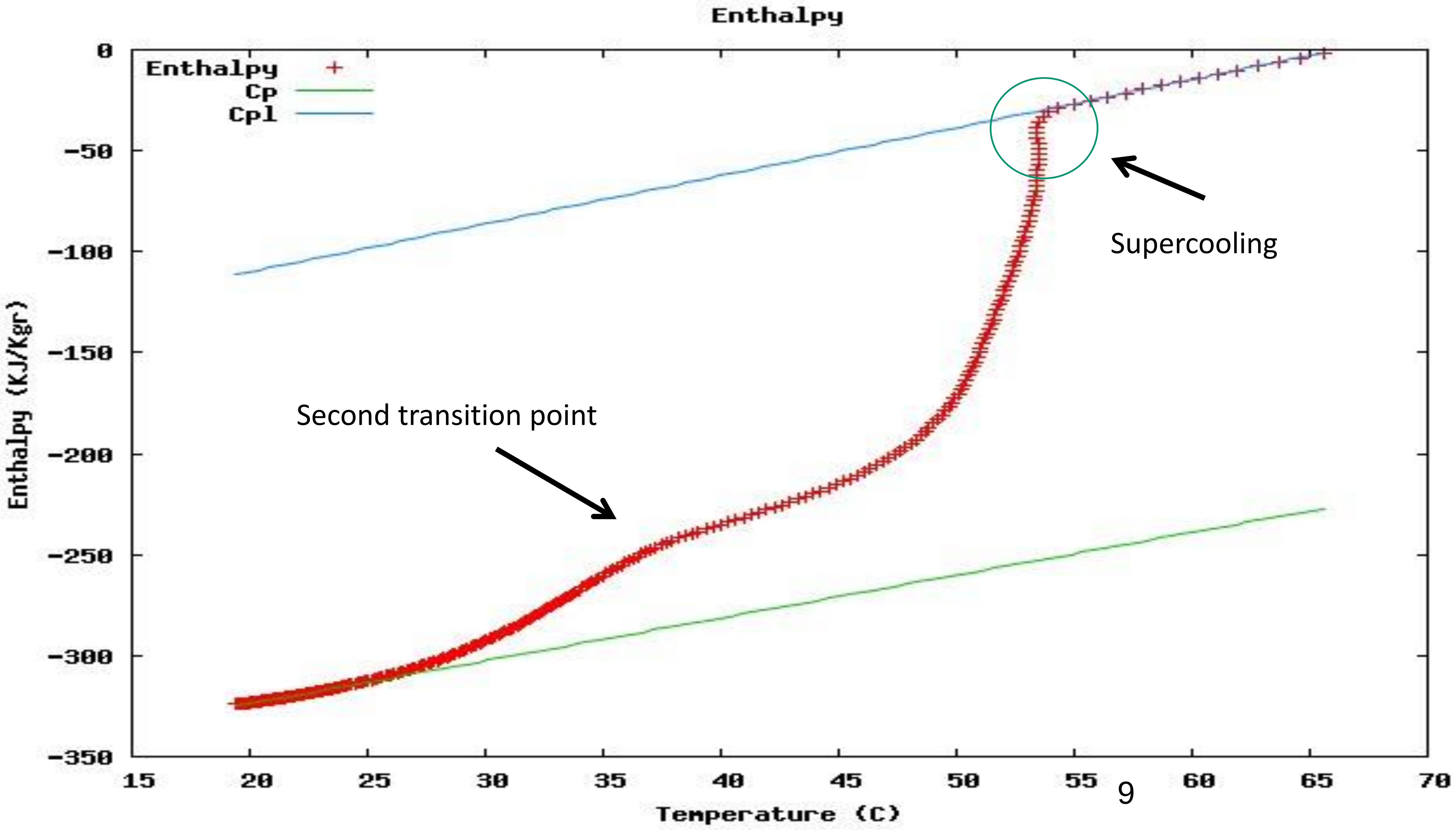

Supercooling

Second transition point

A53 Specific Heat vs Temperature

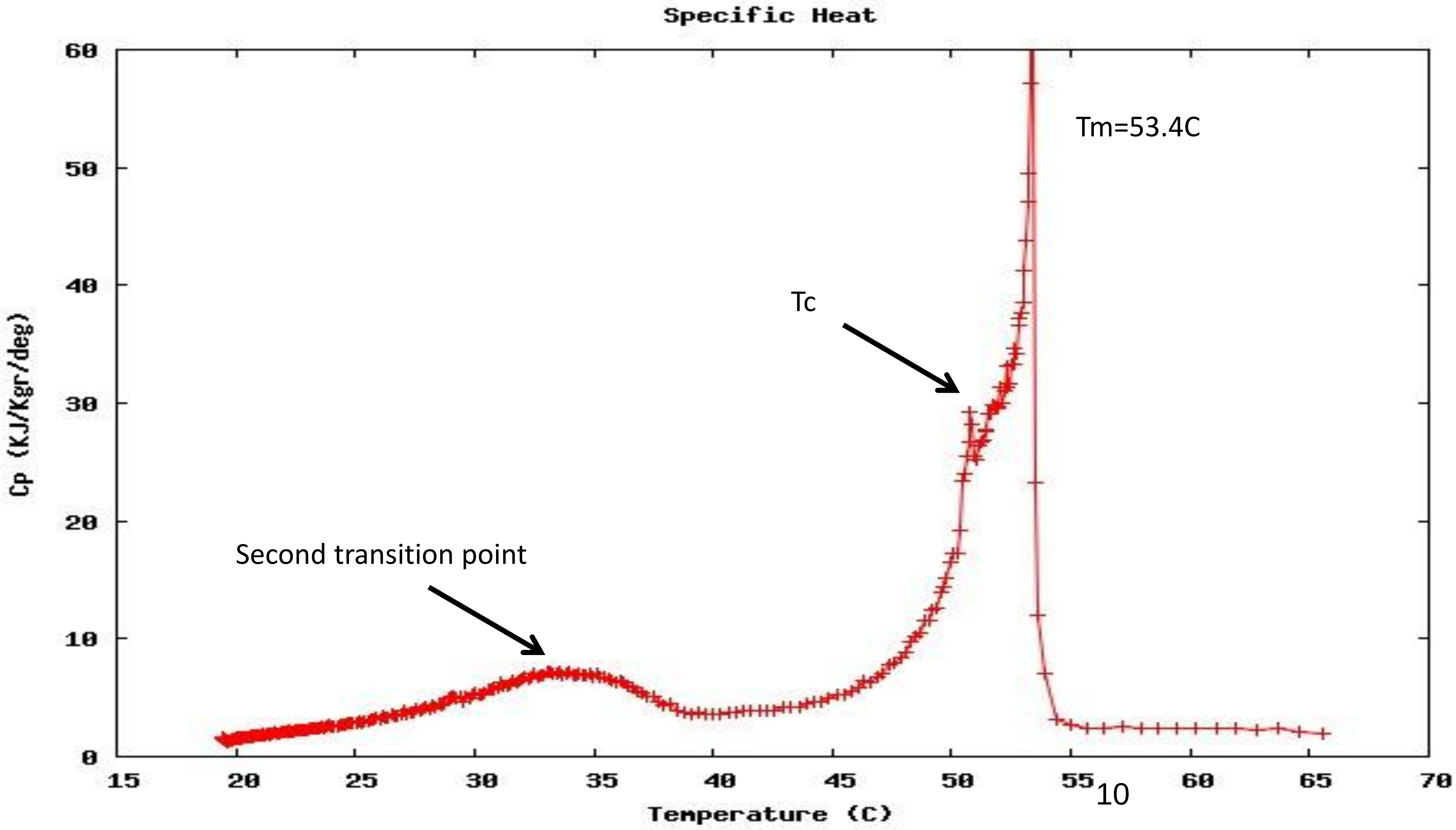

Tm=53.4C

Tc

Second transition point

T-Historv Curve for A58

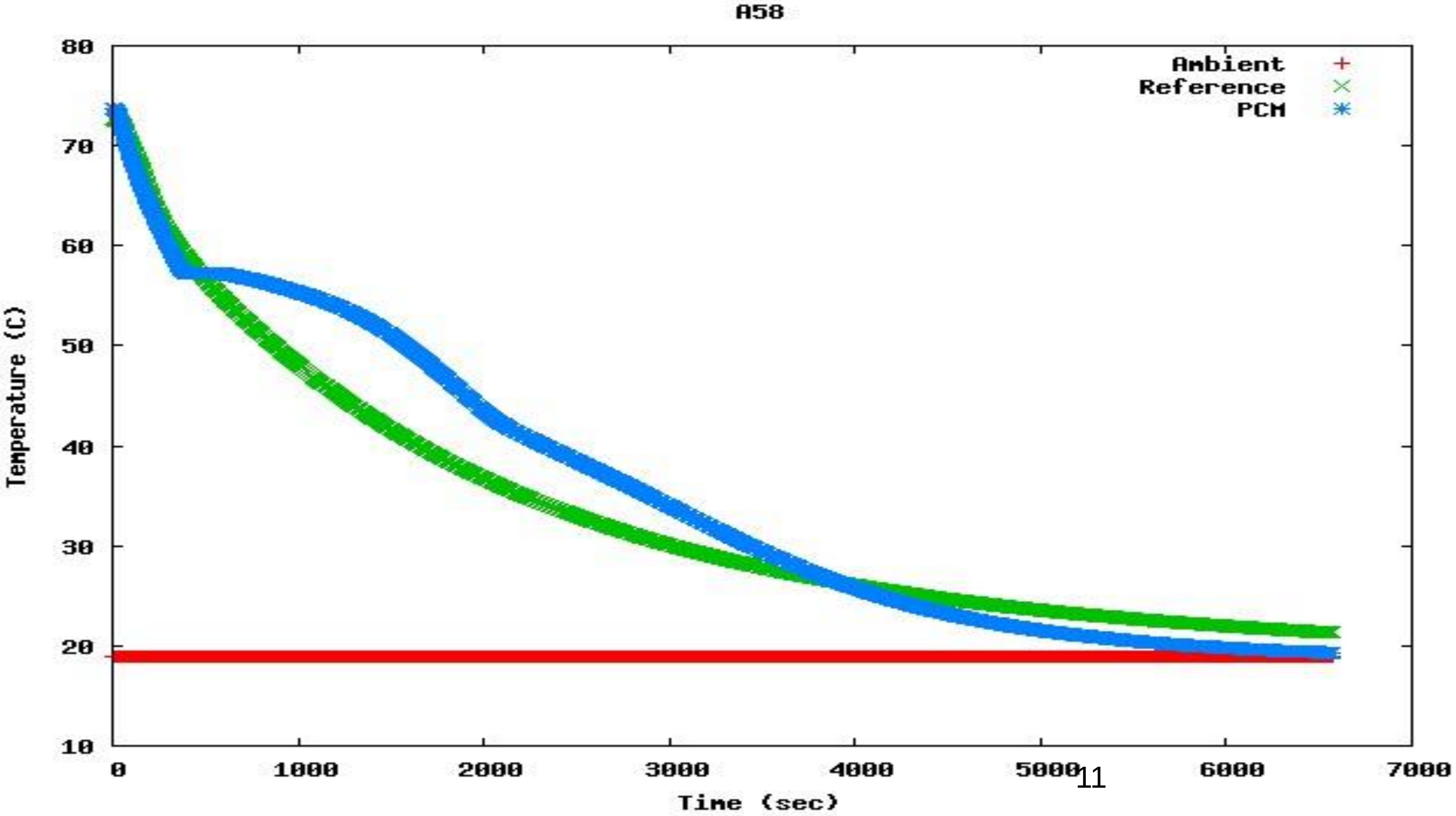

A58: Supercooled region

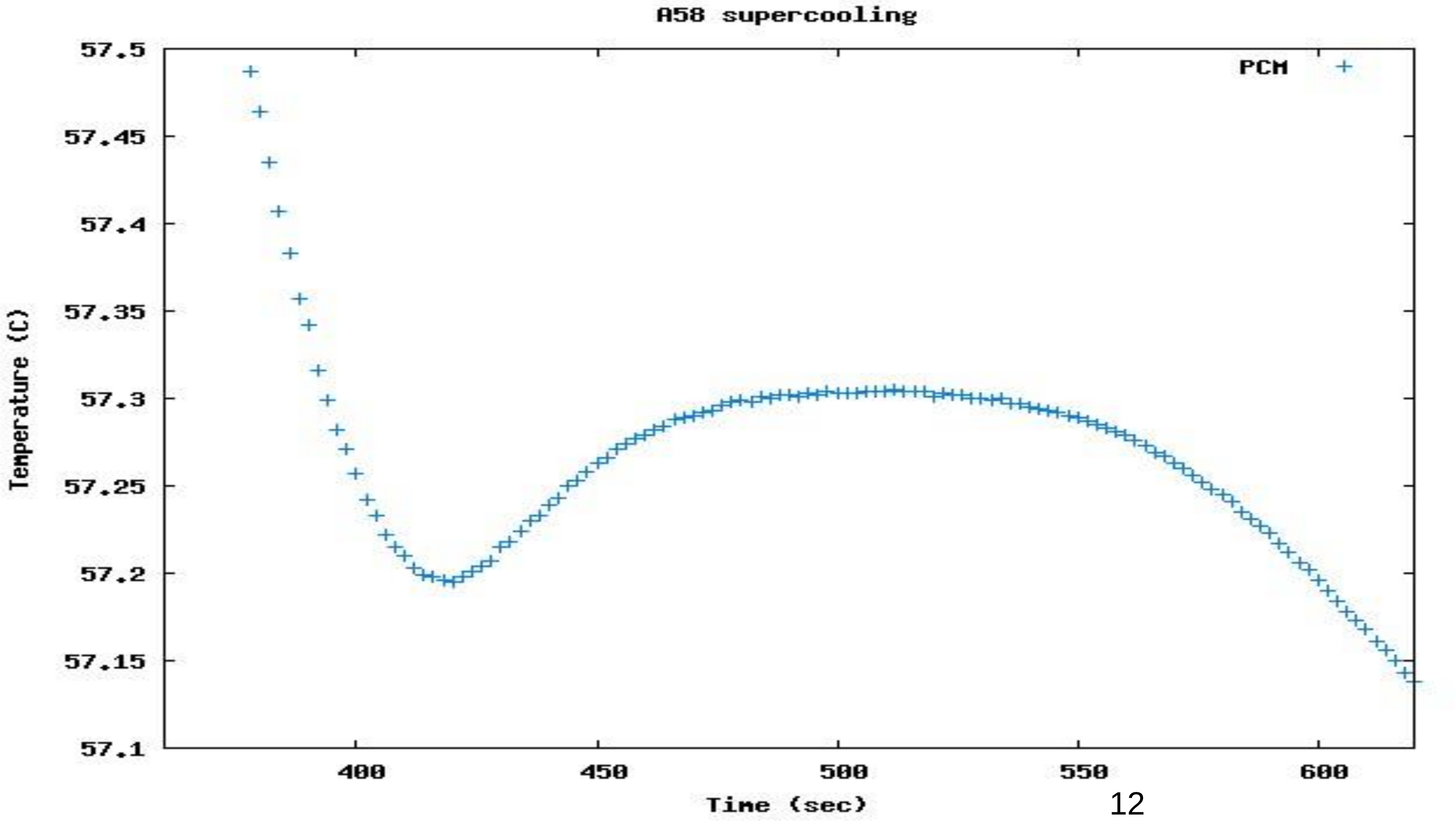

A58: Enthalpy vs Temperature

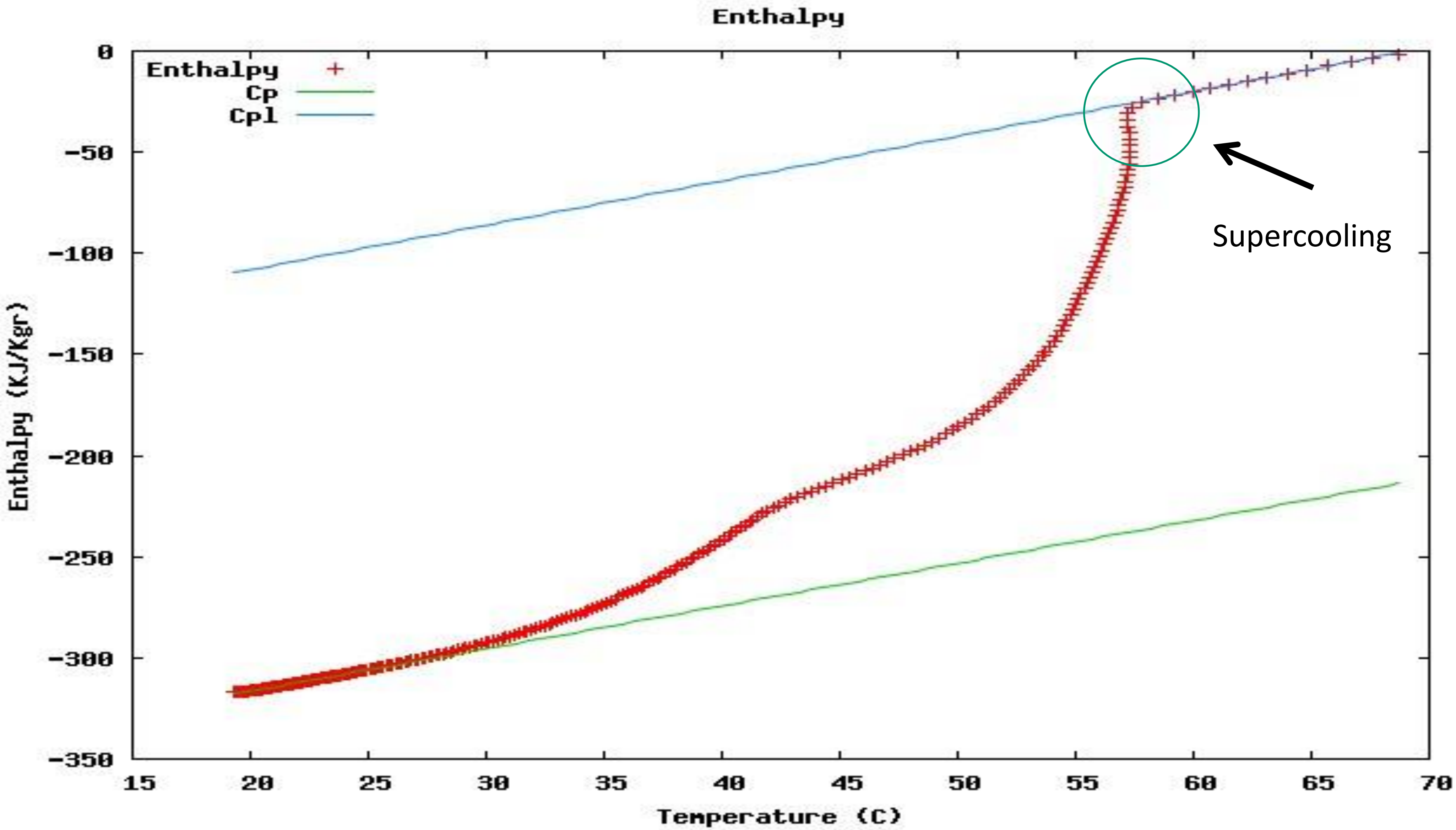

Supercooling

Drawbacks - Solutions

- Ambiguous time limits of the various regions.
- Serious errors in the integrations of the areas determining the heat content of the phases.
- Very sensitive to experimental errors (error by 0.5C may result in 60% error in the Cp or Hm).

Alternative approaches (within the same framework):

- Use of the temperature instead of the time for the definitions of the various regions (phases).
- Integration in the flat regions (e.g. during solidification) undefined.

Decision:

Redesign the experimental procedure considering **numerical solution of the Diffusion Equation** with boundary conditions adapted appropriately to the experimental situation.

Representative case of Capric Acid

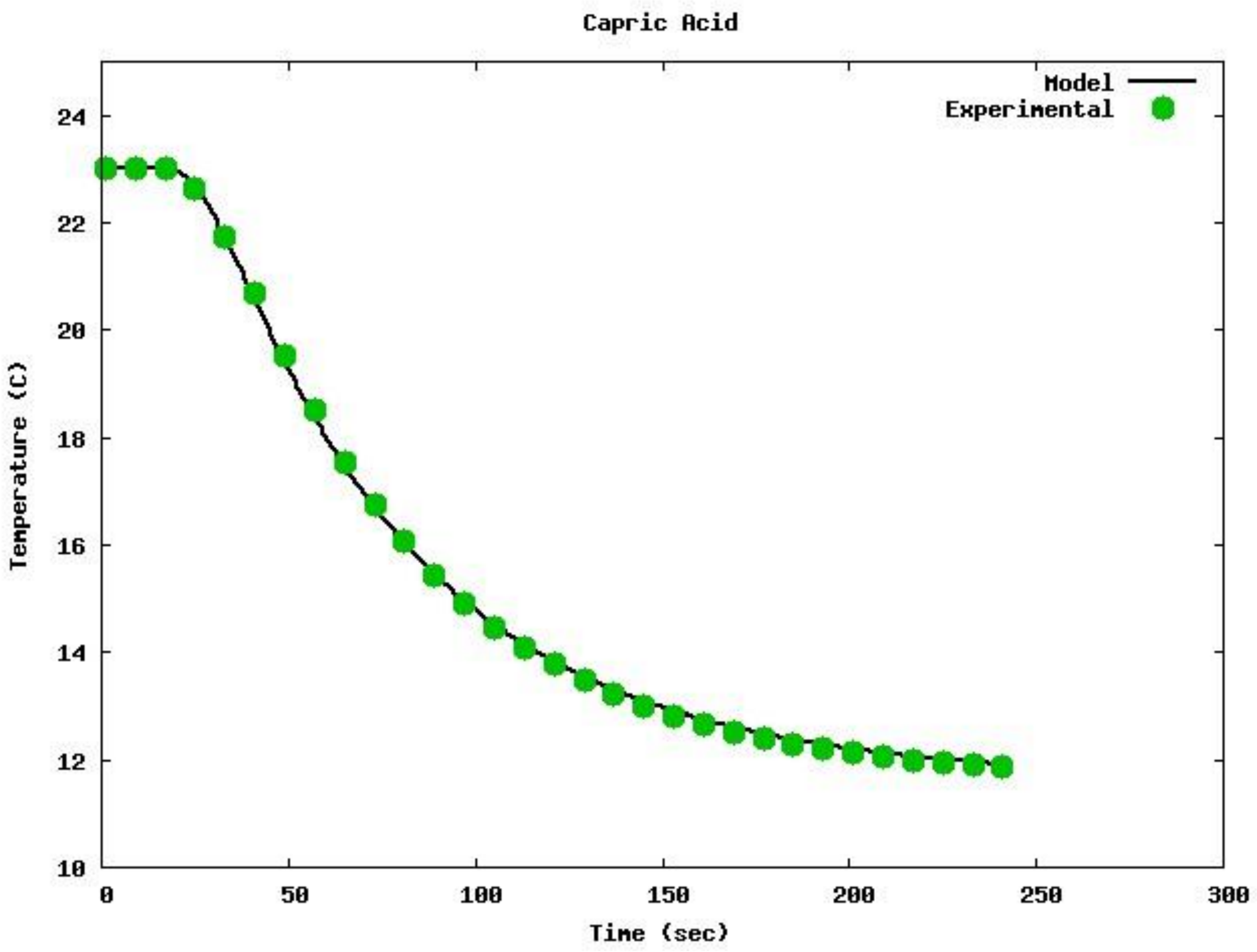

Latent Heat 155KJ/Kg
Specific Heat Cp=2.1KJ/KgK
Thermal Conductivity Ks=0.19W/mK

Good Agreement with literature

Selection of NPs

xGnPs ultrathin particles of graphite or
short stacks of graphene sheets (XG Sciences, Inc.)

Advantages:

- Very high thermal conductivity, k=3,000 W/mK parallel to surface of platelet (k=6 W/mK perpendicular to surface)
- Can easily tailor different dimensions, thickness and shape anisotropies
- Relatively low cost (even easy to produce)
- Environmentally friendly

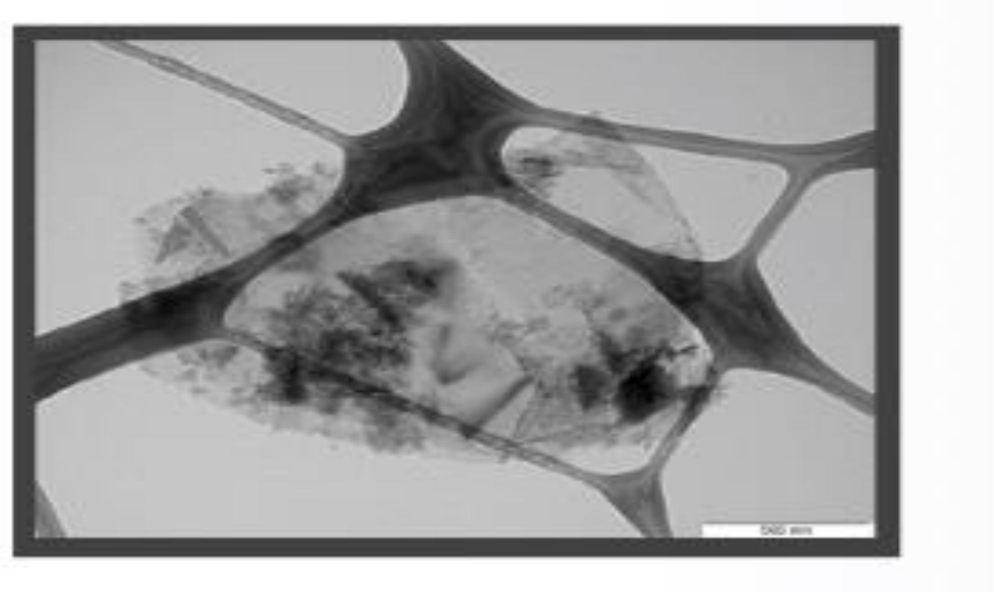

xGnP Grade C

Nps in the form of bulk dry powder:

•Grade M (t=6-8nm, SA=120-150m^2/g, ρ=0.03-0.1g/cm^3):
  - M15 d= 15μm
  - M5 d=5μm

•Grade C aggregates of platelets with ρ=0.2-04g/cm^3):
  - t few nms
  - d<2μm
  - SA=300, 500, 750 m^2/g

•Grade H(t=15nm, SA=50-80m^2/g, ρ=0.03-0.1g/cm$^{3)}$:
  - H5 d=5μm

Specific Heat and latent heat measurements

- We used (in parallel to heat bath and the numerical solution of the THCE) Modulated Differential Scanning Calorimetry (MDSC).
- MDSC differs from standard DSC in that MDSC® uses two simultaneous heating rates - a linear heating rate that provides information similar to standard DSC, and a sinusoidal or modulated heating rate that permits the simultaneous measurement of the sample's heat capacity.

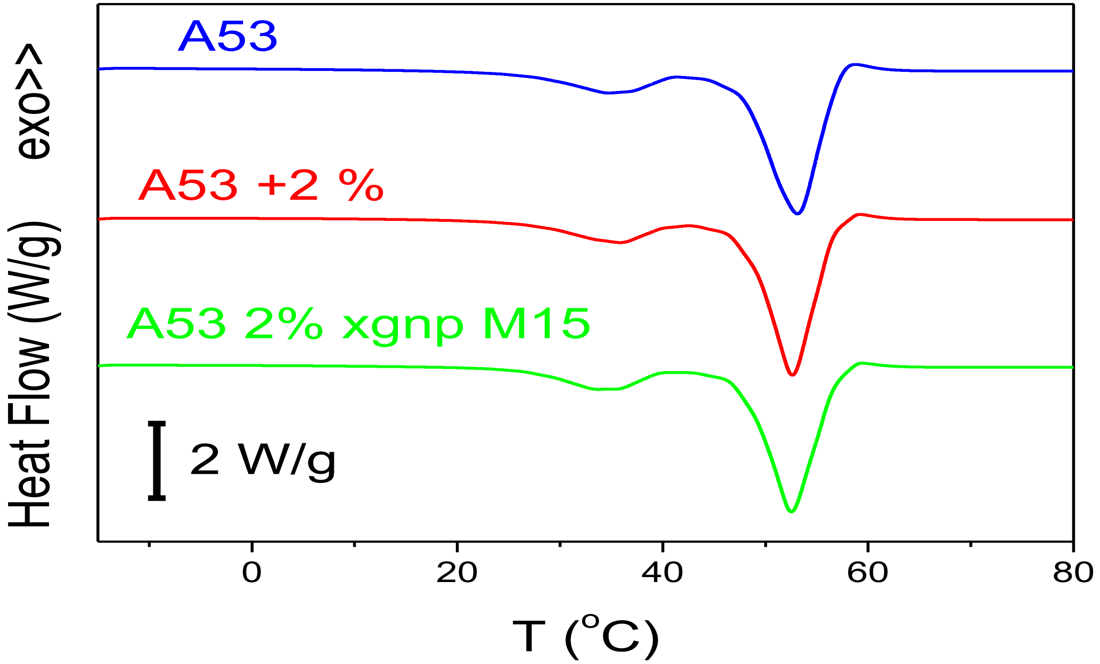

Specific Heat (MDSC) and Latent Heat (DSC)

A53 + M15	C_p^{solid} (J/g°C)				C_p^{liquid} (J/g°C)			**ΔH (J/g)**	**Ks(w/mK)**
	T=5°C	T=10°C	T=15°C	T=20°C	T=70°C	T=75°C	T=80°C		
0%	1.81	1.93	2.08	2.34	2.37	2.38	2.40	195	0.22
0.5%	1.95	2.04	2.18	2.43	2.52	2.54	2.57	191	0.36
1%	1.84	1.95	2.08	2.29	2.38	2.41	2.42	192	0.44
2%	1.78	1.88	1.99	2.21	2.34	2.36	2.37	189	0.33
4%	1.65	1.74	1.86	2.04	2.22	2.24	2.26	180	0.39
6%	1.63	1.71	1.84	2.00	2.20	2.21	2.22	170	0.78
A53 + M5	T=5°C	T=10°C	T=15°C	T=20°C	T=70°C	T=75°C	T=80°C	**ΔH (J/g)**	**Ks(w/mK)**
1%	1.72	1.81	1.93	2.16	2.26	2.28	2.29	188	0.27
2%	1.72	1.80	1.92	2.12	2.26	2.29	2.31	184	0.36
4%	1.67	1.78	1.90	2.08	2.21	2.23	2.26	186	0.43
6%				1.95				190	0.42
A53+C750	5°C	10°C	15°C	20°C	70°C	75°C	80°C	**ΔH (J/g)**	**Ks(w/mK)**
0%	1.81	1.93	2.08	2.34	2.37	2.38	2.40	195	0.22
1%	1.79	1.89	2.03	2.27	2.38	2.40	2.41	189	0.26
2%	1.80	1.88	2.02	2.26	2.38	2.40	2.41	183	0.25
4%	1.68	1.76	1.89	2.10	2.20	2.21	2.22	179	0.26

Specific Heat (MDSC) and Latent Heat (DSC)

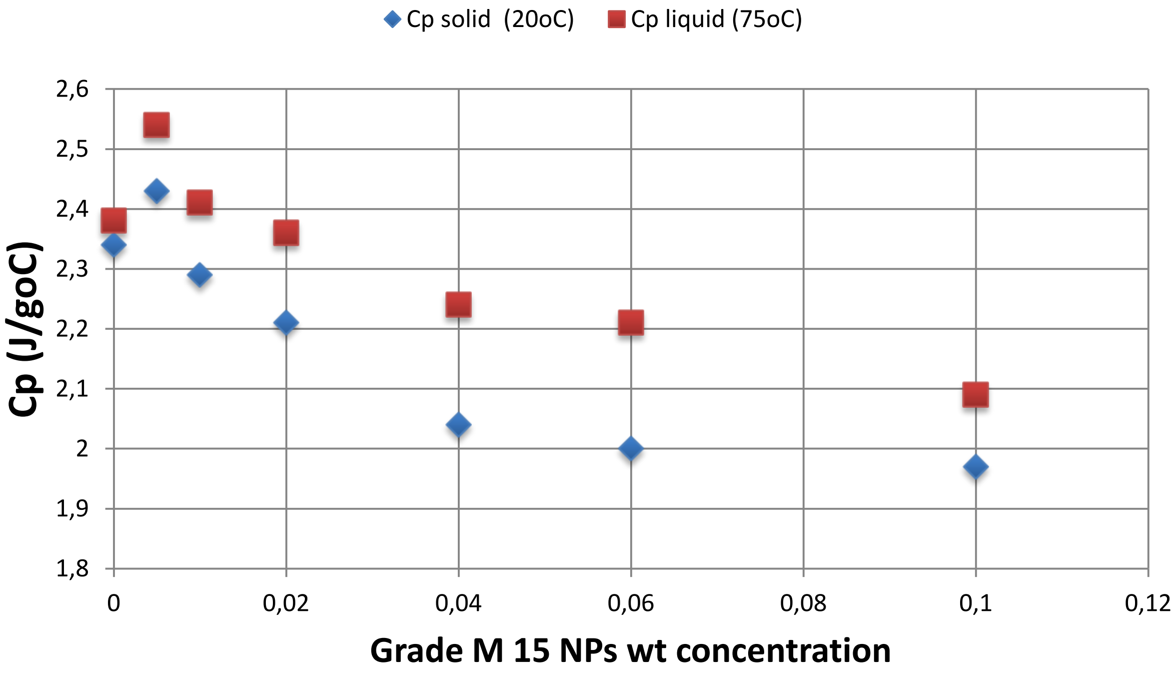

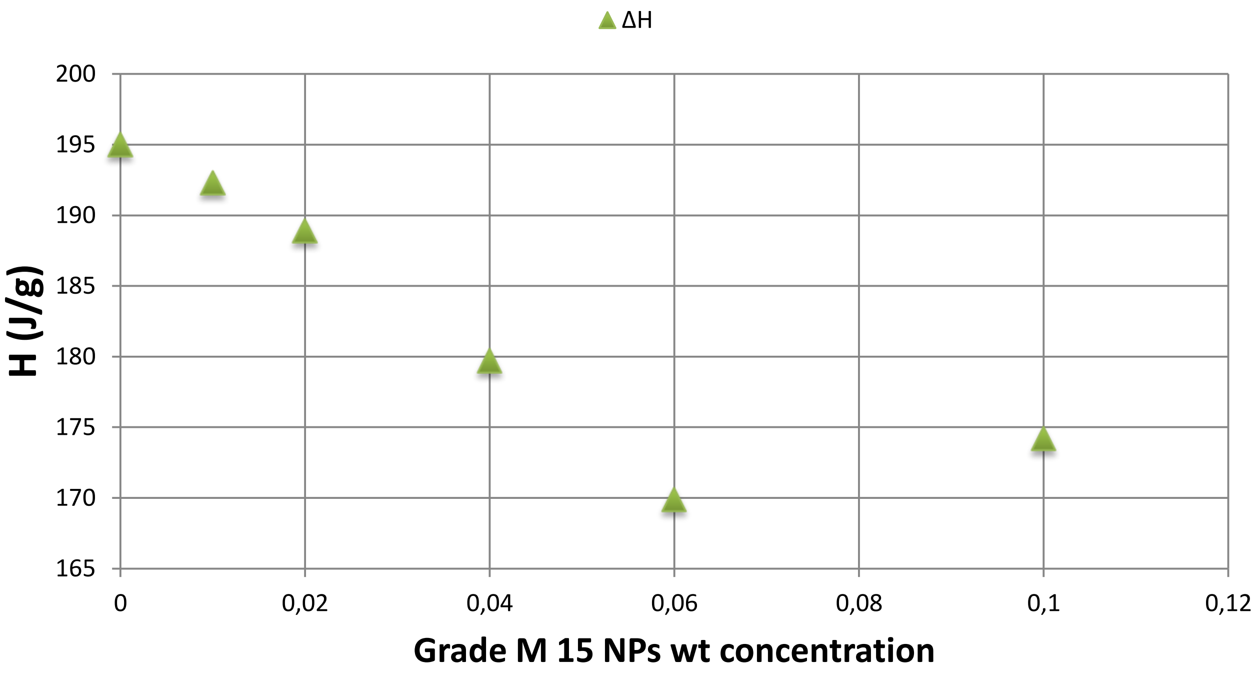

Thermal conductivity of A53 with graphite nano-paletelets as a function of weight fraction with different sizes, aspect ratios and surface areas.

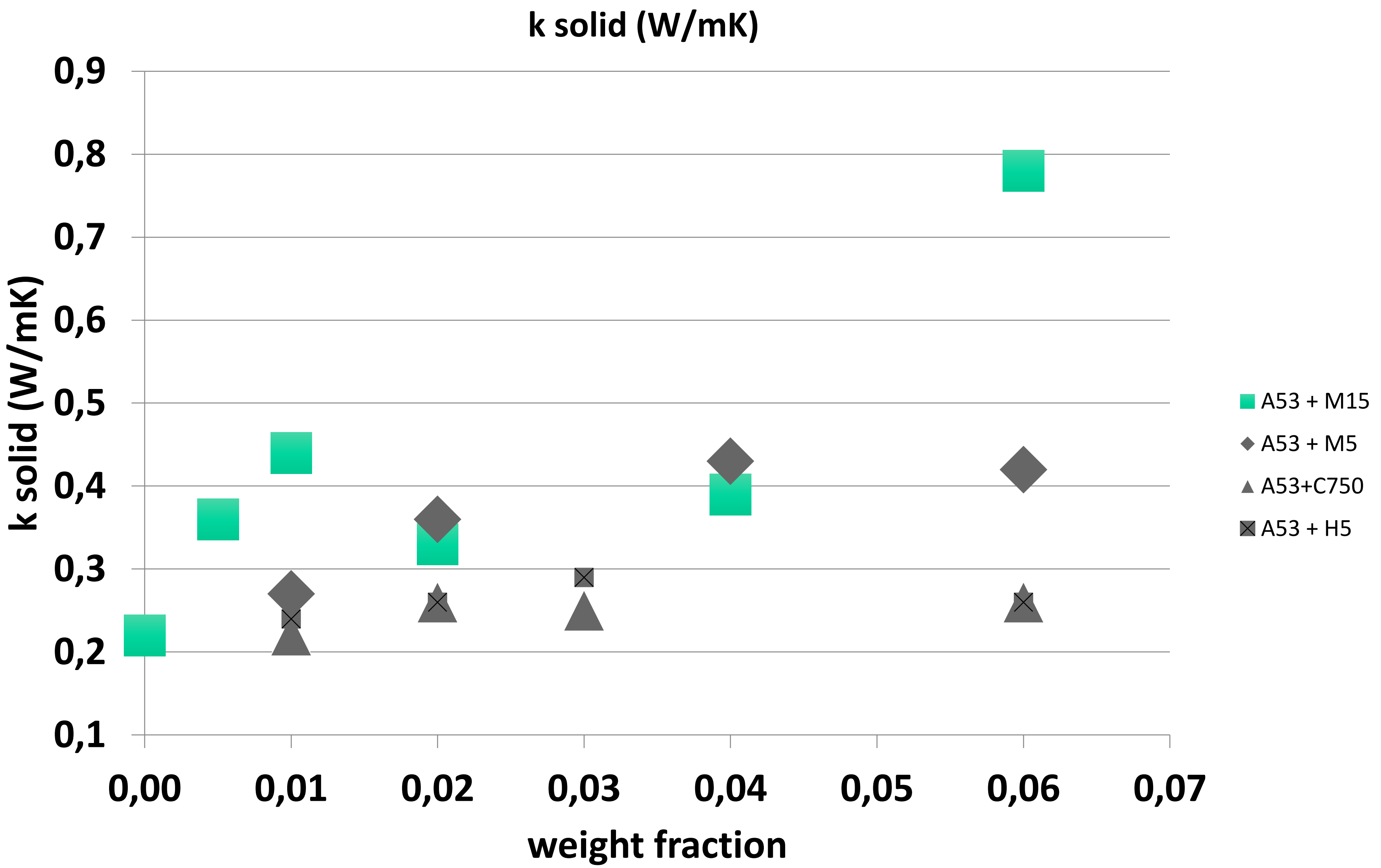

6/30/2017

The case of A44

A44+M5	Cp (KJ/Kgdeg)	H(KJ/Kg)	Ks (w/mK)
0%	1.85±0.15	250±10	0.41±0.05
1%	1.53	252	0.37
2%	1.56	247	0.46
3%	1.73	241	0.61

Conclusions on Thermal conductivity of composites A53+ graphite nano-platelets (xGnP)

- M15 and M5 NPs, differ only in the diameter d=15 and 5μm, respectively
- Grade C is overall smaller than Grade M, but with larger surface area
- (M15) d=15μm and t=6-8nm, Surface Area=120-150m2/g
- (M5) d=5μm and t=6-8nm, Surface Area=120-150m2/g;
- (H5) d=5μm t=15nm, Surface Area=50-80m2/g);
- (C750) d<2μm, t a few nm and surface area=750 m2/g.

CONCLUSION: The **aspect ratio** of the NPs is of importance; in the case of **M15**, which has the **smallest** one, the thermal conductivity **increases** by more than **2 times** upon 1% additions.

- Development of a ALN based thin film to protect the HEs metal surface from the corrosion of Hydrated salts

PCM encapsulation and integration in metallic components

Plates and vessels filled


(Rubitherm GmbH)


(Cool Desck 24)

Internal blinds

F. Souayfane et al., Energy Build. 129 (2016) 396–431

Aluminium profiles with fins

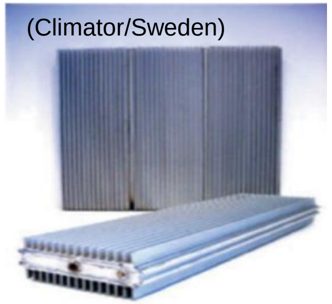
(Climator/Sweden)

H. Mehling, & L.F. Cabeza LF. Kluwer Academic Publishers Group (2007)

Storage units and tanks


F. Rouault et al., Appl. Energy 111 (2013) 1099–1106


A. Gil et al., Int. J. Refrig. 39 (2014) 95–103

Heat exchangers with integrated fins for improved heat transfer


Fins: Stainless steel 304 L

A. Gil et al., Int. J. Refrig. 39 (2014) 95–103


L.F. Cabeza et al., Renew. Sustain. Energy Rev. 15 (2011) 1675–1695

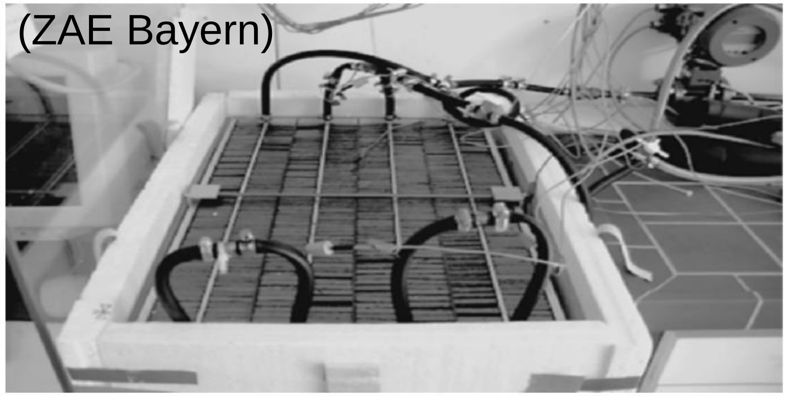
(ZAE Bayern)

H. Mehling, & L.F. Cabeza LF. Kluwer Academic Publishers Group; 2007

Need for corrosion protection of metallic components from salt hydrate PCM

Introduction

Anticorrosive protective coating

Fulfilments

- High thermal conductivity
- Mechanical strength
- Industrial scale production

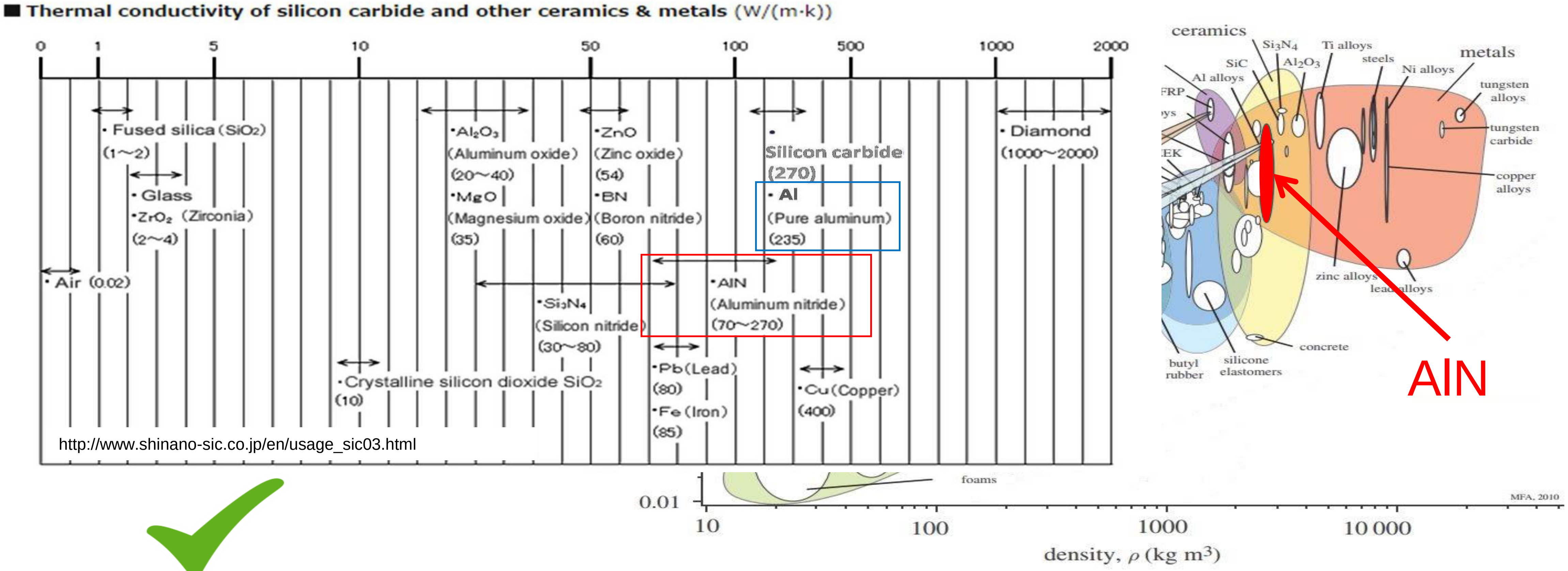

http://www.shinano-sic.co.jp/en/usage_sic03.html

✓

N.A. Fleck et al., Proc. R. Soc. A 466 (2010) 2495–2516

Experimental details

Reactive magnetron sputtering

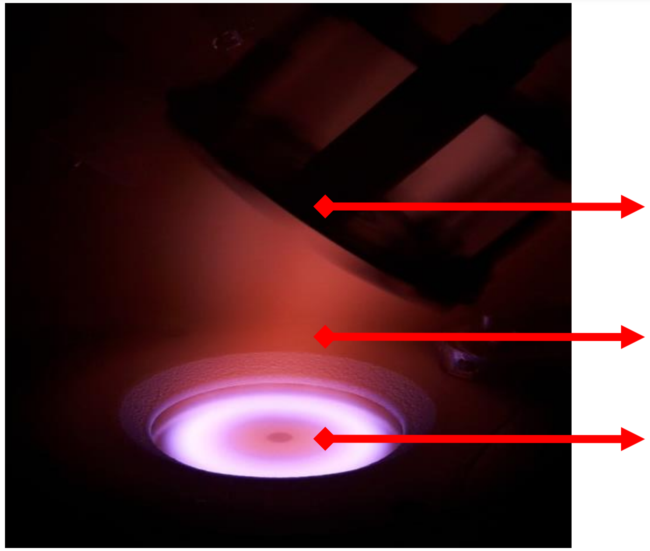

$P_b = 5x10^{-6}$ mbar

Rotating substrate:
Commercial Al (1050) sheet
(non treated)

Ar/N_2 atmosphere

Al target (purity 99.99%)

AlN/Al

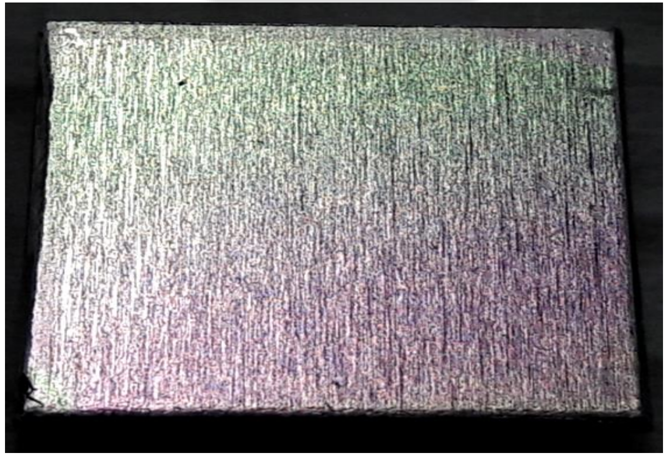

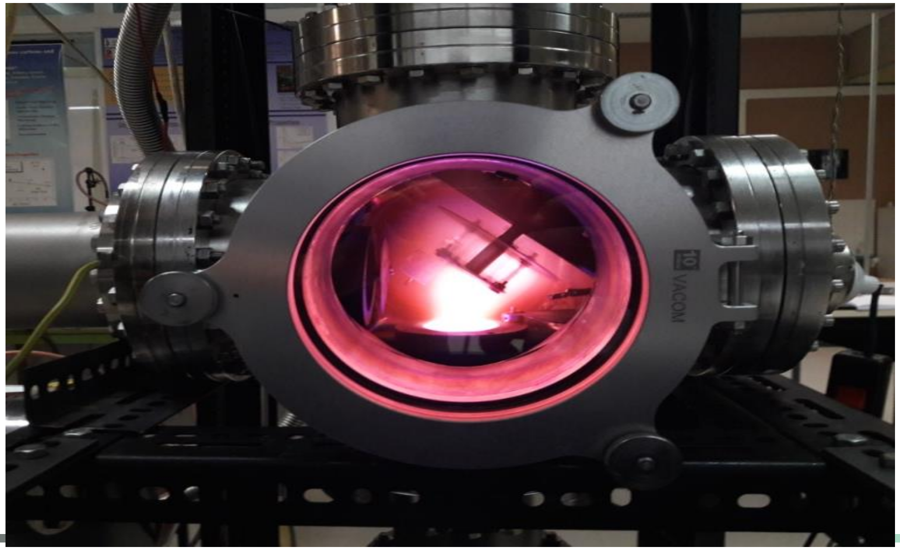

XRR
XRD
XPS
SEM
Corrosion tests

Results

Corrosion behaviour of AlN/Al films in highly aggressive environment

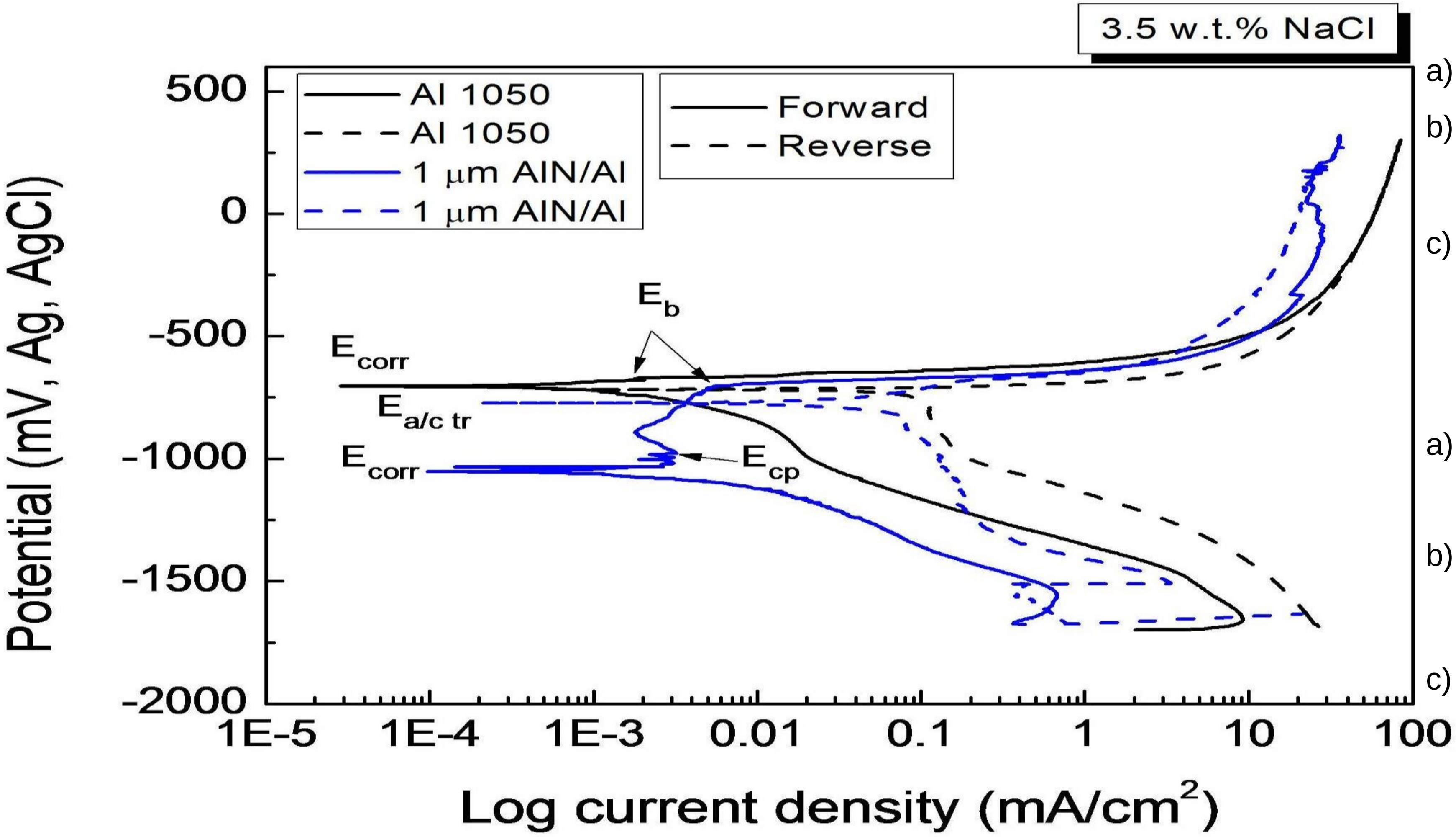

CP-Al1050

a) No passivity is observed

b) Sustained flat gradient of the polarization curve immediately after E_{corr}

c) Negative hysteresis

Pitting

AlN/Al

a) Passivity occurs over a notable range of anodic potentials (E_b-E_{cp}=~300 mV)

b) Passive currents lower than 0.1 mA/cm^2 (i_p=0.003 mA/cm^2)
➔ True passivity

c) Nobler $E_{a/c\ tr}$ compared to E_{corr}

True passivity - Nobler surface

Results

Corrosion behaviour of AlN/Al films in PCM

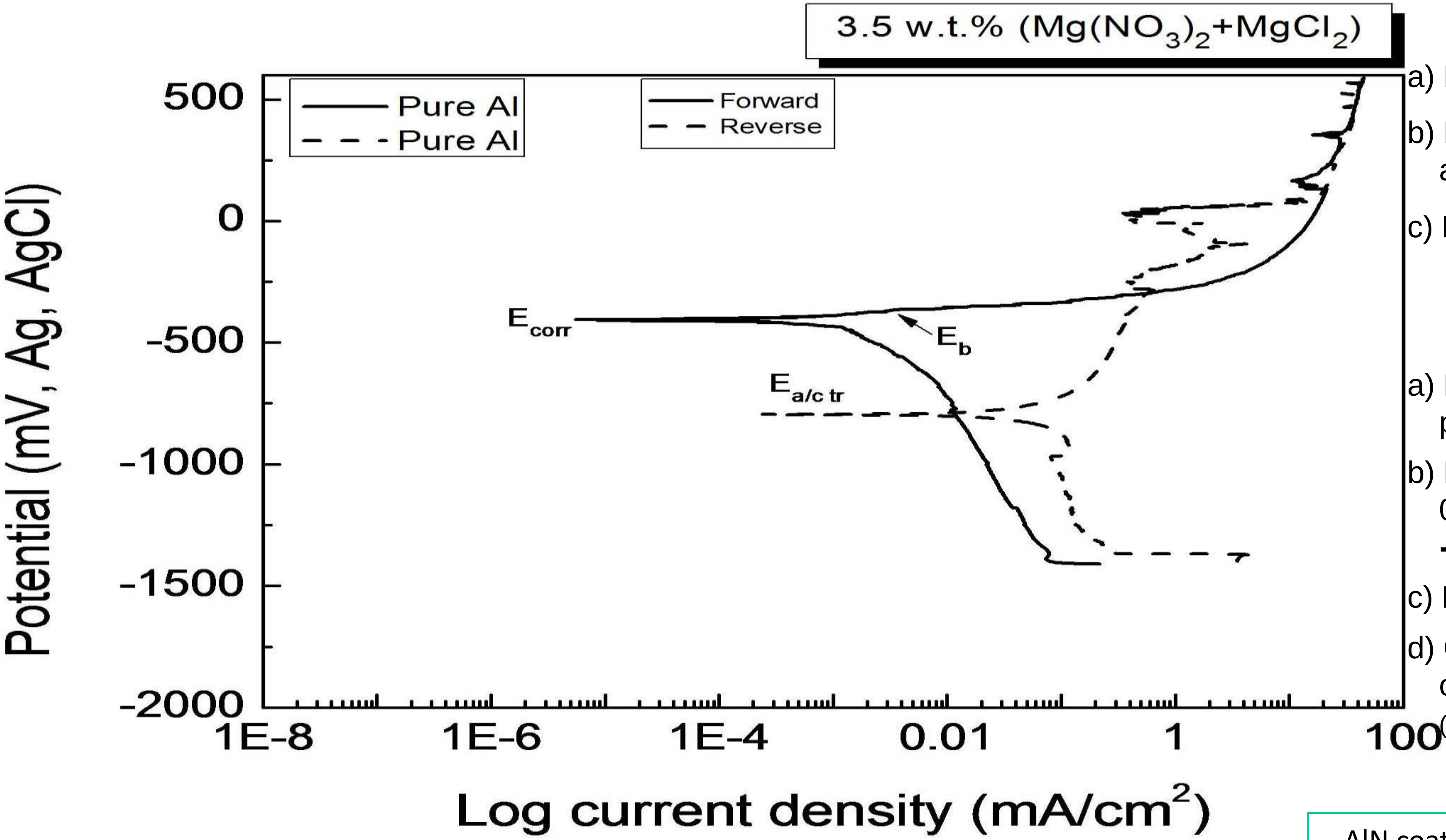

CP-Al 1050

a) No passivity is observed

b) Extended flat gradient of the polarization curve after E_{corr}

c) Lower $E_{a/c\ tr}$ compared to E_{corr}

Pitting

AlN/Al

a) Passivity occurs over a large range of anodic potentials (E_b-E_{cp}=~710 mV)

b) Passive currents lower than 0.1 mA/cm^2(i_p=0.00023 mA/cm^2)
➔ True passivity

c) Nobler $E_{a/c\ tr}$ compared to E_{corr}

d) Corrosion current density of almost one order of magnitude lower compared to CP Al
(i^{AlN}_{corr}= 0.0002 mA/cm^2, i^{Al}_{corr}= 0.003 mA/cm^2)

AlN coatings shows true passivity and superior uniform corrosion performance

TESSE2B
the smart energy storage

Thank for your attention

UOI

Thermal Energy
Storage Systems

for energy efficient building an integrated solution for residential building
energy storage by solar and geothermal resources

European
Commission